Phosphine-Rh_2[(*R*)-MTPA]$_4$ Adducts in Solution: Characterization by NMR Spectroscopy and Chiral Discrimination

Damian Magiera,[§] Jan Omelanczuk,[†] Kamil Dziuba,[‡] K. Michał Pietrusiewicz,*[,‡,#] and Helmut Duddeck*[,§]

Institut für Organische Chemie, Universität Hannover, Schneiderberg 1B, D-30167 Hannover, Germany, Centre of Molecular and Macromolecular Studies, Department of Organic Sulfur Compounds, Polish Academy of Sciences, PL-90-363 Łódź, Sienkiewicza 112, Poland, Department of Organic Chemistry, Maria Curie-Sklodowska University, Lublin, Poland, and Institute of Organic Chemistry, Polish Academy of Sciences, ul. Kasprzaka 44/52, PL-01-224 Warsaw, Poland

Received November 18, 2002

The adducts of dirhodium tetraacylates and phosphines are characterized in solution by ^{1}H and ^{31}P NMR spectroscopy at room temperature. A differentiation of the enantiomers of chiral phosphine ligands is easily performed by NMR signal integration after adduct formation with the enantiopure Rh_2[(*R*)-(+)-MTPA]$_4$ complex (**Rh***). Stereochemical aspects are discussed in terms of chiral discrimination and adduct diastereomerism. A second type of chiral recognition was discovered, namely, that between two ligand molecules in 2:1 adducts across the Rh_2[(*R*)-(+)-MTPA]$_4$ building block. Conditions for optimizing the experiment for the determination of enantiomeric composition of chiral phosphines by the "dirhodium method" are presented. The possibility of determining absolute configurations of chiral phosphines is briefly discussed.

Introduction

Dirhodium and other dinuclear complexes have been studied intensively during the last few decades.[1] They were applied frequently as homogeneous catalysts[2] and as auxiliaries in the chirality determination of compounds with various functional groups by circular dichroism.[3] It should be mentioned that dirhodium complexes are even in the focus of medicinal interest.[4]

In a series of papers[5] we have studied the potential of the dirhodium complex Rh_2[(*R*)-(+)-MTPA]$_4$ [**Rh***, MTPA-H = methoxytrifluoromethylphenylacetic acid ≡ Mosher's acid; Scheme 1, top] as a solvating agent for the determination of enantiomeric ratios of various chiral monofunctional ligands. It has been shown that the "dirhodium method" is particularly suitable for soft-base functionalities where the classical method of chiral lanthanide shift reagents (CLSR)[6] usually fail. Typically, **Rh*** and ligands form kinetically labile adducts so that only averaged NMR signals can be observed for the ligand molecules in the room-temperature equilibria (in analogy to the CLSR method).

In contrast to previously studied ligands (olefins, epoxides, nitriles, sulfoxides, iodides, phosphine chalcogenides, and selenides),[5,7] phosphines form adducts[8] in solution that are kinetically stable on the NMR timescale (Scheme 1, center), even at room temperature.[9] Such unusual behavior of phosphine ligands has been noticed before by Drago et al.[10] using achiral molecular systems (see below).

Results and Discussion

The assignments of the ^{1}H and ^{13}C NMR signals of the phosphine ligands **1**−**7** (Schemes 1, bottom, and 2)

* To whom correspondence should be addressed. (H.D.) Tel: +49 511 762 4615. Fax: +49 511 762 4616. E-mail: duddeck@mbox.oci.uni-hannover.de. (M.P.) Tel: +48 81 537 5679. Fax: +48 81 524 2251. E-mail: michal@hermes.umcs.lublin.pl.

§ Hannover University.

† Centre of Molecular and Macromolecular Science.

‡ Maria Curie-Sklodowska University.

Polish Academy of Sciences.

(1))(a) *Multiple Bonds between Metal Atoms*, 2nd ed.; Cotton, F. A., Walton, R. A., Eds.; Clarendon: Oxford, 1993. (b) Boyar, E. B.; Robinson, S. D. *Coord. Chem. Rev.* **1983**, *50*, 109−208.

(2)) (a) Mertis, C.; Kravaritoy, M.; Chorianopoulou, M.; Koinis, S.; Psaroudakis, N. *Top. Mol. Org. Eng.* **1994**, *11*, 321−329. (b) *Modern Catalytic Methods for Organic Synthesis with Diazo Compounds: From Cyclopropanes to Ylides*; Doyle, M. P., McKervey, M. A., Ye, T., Eds.; Wiley: New York, 1998. (c) Endres, A.; Maas, G. *Tetrahedron* **2002**, *58*, 3999−4005, and references therein.

(3) For example: (a) Snatzke, G.; Wagner, U.; Wolff, H. P. *Tetrahedron* **1981**, *37*, 349−361. (b) Gerards, M.; Snatzke, G. *Tetrahedron: Asymmetry* **1990**, *1*, 221−236. (c) Cotton, F. A.; Falvello, L. R.; Gerards, M.; Snatzke, G. *J. Am. Chem. Soc.* **1990**, *112*, 8979−8980. (d) Frelek, J.; Szczepek, W. J. *Tetrahedron: Asymmetry* **1999**, *10*, 1507−1520.

(4) Clarke, M. J.; Zhu, F.; Frasca, D. R. *Chem. Rev.* **1999**, *99*, 2511−2533.

(5) (a) Wypchlo, K.; Duddeck, H. *Tetrahedron Asymmetry* **1994**, *5*, 27−30. (b) Wypchlo, K.; Duddeck, H. *Chirality* **1997**, *9*, 601−603. (c) Hameed, S.; Ahmad, R.; Duddeck, H. *Magn. Reson. Chem.* **1998**, *36*, S47−S53. (d) Meyer, C.; Duddeck, H. *Magn. Reson. Chem.* **2000**, *38*, 29−32. (e) Rockitt, S.; Duddeck, H.; Omelanczuk, J. *Chirality* **2001**, *13*, 214−223. (f) Malik, S.; Duddeck, H.; Omelanczuk, J.; Choudhary, M. I. *Chirality* **2002**, *14*, 407−411.

(6) (a) Sullivan, G. R. *Top. Stereochem.* **1978**, *10*, 287−329. (b) Rinaldi, P. L. *Prog. NMR Spectrosc.* **1983**, *15*, 291−352. (c) Parker, D. *Chem. Rev.* **1991**, *91*, 1441−1457. (d) Rothchild, R. *Enantiomer* **2000**, *5*, 457−471.

(7) Duddeck, H.; Malik, S.; Gáti, T.; Tóth, G.; Choudhary, M. I. *Magn. Reson. Chem.* **2002**, *40*, 153−156.

(8) For the solid state structures of the 2:1 adducts of **Rh-TFA** with PPh_3 and $P(OPh)_3$ ligands see: Cotton, F. A.; Felthouse, T. R.; Klein, S. *Inorg. Chem.* **1981**, *20*, 3037−3042.

(9) Magiera, D.; Baumann, W.; Podkorytov, I. S.; Omelanczuk, J.; Duddeck, H. *Eur. J. Inorg. Chem.* **2002**, 3253−3257.

(10) 0) (a) Telser, J.; Drago, R. S. *Inorg. Chem.* **1984**, *23*, 2599−2606. (b) Telser, J.; Drago, R. S. *Inorg. Chem.* **1986**, *25*, 2989−2992.

10.1021/om0209529 CCC: $25.00
Publication on Web 05/16/2003

Scheme 1. Structures of the Dirhodium Complexes (top), Equilibria of Free Rh* and Its Phosphine Adducts (center), and the Achiral Phosphines 1−3 (bottom)[a]

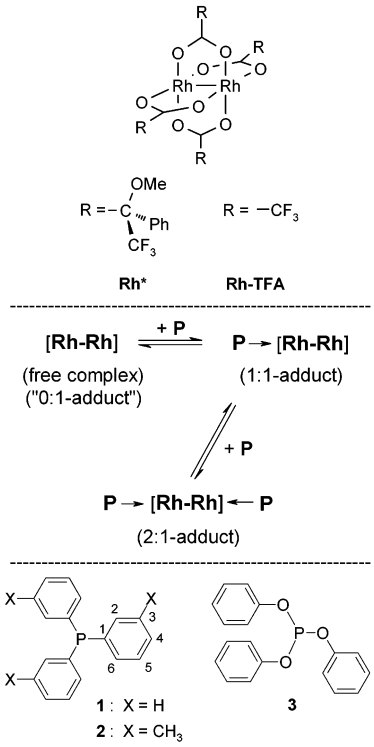

[a] In the formula schemes the chiral dirhodium complex **Rh*** is represented by "[**Rh-Rh**]" and the phosphine ligands by "**P**" or by their compounds numbers **1**−**7**.

were straightforward on the basis of literature data.[11] The ^{1}H signals were sometimes complex and overlapping, especially for phenyl groups attached to P. A particularly severe case is triphenylphosphine (**1**), so that we included tris(3-methylphenyl)phosphine (**2**) in our study in which the signals are much more dispersed but the spin−spin coupling parameters are expected to be very similar to those of **1**. Likewise, ^{13}C signals of pentafluorophenyl groups were obscured due to the manifold ^{19}F,^{13}C couplings. All NMR data of the free ligands and their 1:1 adducts are collected in Tables 1−7.

(I) Achiral Phosphines: Adduct Formation. As noted before,[9,10] phosphines are unique in forming adducts with dirhodium tetraacylates whose lifetimes are long enough to observe the individual adducts by solution NMR at room temperature ("frozen equilibria"). Moreover, they provide ^{31}P signal splittings due to scalar ^{103}Rh,^{31}P coupling.[9,10b] Therefore, we regarded it necessary first to explore suitable experimental conditions for recording the NMR data of adducts with a variety of structurally different phosphines (e.g., **1**−**7**). To this end, we started by investigating the mode of adduct formation and performed NMR titration experiments varying the molar ratios of the phosphines **1** and **3** (symbol **P** in Scheme 1, center) and the dirhodium complex **Rh*** (symbol [**Rh**−**Rh**]) from 1:1 (excess of rhodium sites) to 2:1 (equal number of phosphorus and rhodium sites) and further to 3:1 (excess of phosphorus sites).

In the case of PPh_3 (**1**) the adducts are formed consecutively. Using a 1:1 molar ratio, only the ^{31}P signal of the 1:1 adduct appears at $\delta = -35.3$ as a double doublet due to the one- and two-bond couplings of ^{31}P to ^{103}Rh (Figure 1, top). The second molar equivalent of **1** is used for converting the 1:1 into the 2:1 adduct (Figure 1, center), the ^{31}P signal forming the AA′ part

Table 1. ^{1}H, ^{13}C, and ^{31}P Chemical Shifts (δ, in ppm), Coupling Constants $^nJ(^{31}P,X)$ (in Hz) of Free PPh_3 (1) and of the Adduct Rh*←1 (1:1 molar ratio of the components), and Adduct Formation Shifts ($\Delta\delta$, in ppm), in $CDCl_3$

		free ligand		ligand in the adduct		
X		δ	$^nJ(^{31}P,X)$	δ	$^nJ(^{31}P,X)$	$\Delta\delta$
^{1}H	2/6	arom. H: 7.35−7.28	n.d.[a]	7.59	$^3J = 10.7$	∼+0.3
	3/5		n.d.	≈ 7.23	n.d.	∼−0.1
	4		n.d.	7.42	$^5J = 0-2$	∼+0.1
^{13}C	1	137.3	$^1J = 10.8$	130.2	$^1J = 33.4$	−7.1
	2/6	133.7	$^2J = 19.4$	134.4	$^2J = 10.6$	+0.7
	3/5	128.5	$^3J = 7.0$	128.9	$^3J = 9.8$	+0.4
	4	128.7	$^4J \leq 1$	130.6	$^4J \leq 3$	+1.9
^{31}P		−4.2		−35.3	$^1J_{RhP} = 96.1$ $^2J_{RhP} = 23.3$	−31.1

[a] n.d.: not determined due to signal overlap or signal complexity.

Table 2. ^{1}H, ^{13}C, and ^{31}P Chemical Shifts (δ, in ppm), Coupling Constants $^nJ(^{31}P,X)$ (in Hz) of Free (*m*-Tol)$_3$P (2) and of the Adduct Rh*←2 (1:1 molar ratio of the components), and Adduct Formation Shifts ($\Delta\delta$, in ppm), in $CDCl_3$

		free ligand		ligand in the adduct		
X		δ	$^nJ(^{31}P,X)$	δ	$^nJ(^{31}P,X)$	$\Delta\delta$
^{1}H	2	7.17	$^3J = 8.5$	7.44	$^3J = 11.1$	+0.27
	4	7.13	$^5J \leq 1$	7.21	$^5J \leq 1$	+0.08
	5	7.21	$^4J = 1.5$	7.07	$^4J = 2.3$	−0.14
	6	7.06	$^3J = 7.4$	7.36	$^3J = 9.1$	+0.30
	CH_3	2.29	$^5J \leq 1$	2.18	$^5J \leq 1$	−0.11
^{13}C	1	137.1	$^1J = 9.8$	129.9	$^1J = 33.3$	−7.2
	2	134.5	$^2J = 22.3$	134.4	$^2J = 10.8$	−0.1
	3	137.9	$^3J = 7.7$	138.3	$^3J = 9.8$	+0.4
	4	129.5	$^4J \approx 0$	131.0	$^4J = 2.6$	+0.5
	5	128.3	$^3J = 6.5$	128.3	$^3J = 10.3$	0
	6	130.7	$^2J = 16.6$	131.2	$^2J = 9.8$	+0.5
	CH_3	21.4	$^4J \approx 0$	21.2	$^4J \approx 0$	−0.2
^{31}P		−3.9		−34.0	$^1J_{RhP} = 96.3$ $^2J_{RhP} = 23.1$	−31.1

Table 3. ^{1}H, ^{13}C, and ^{31}P Chemical Shifts (δ, in ppm), Coupling Constants $^nJ(^{31}P,X)$ (in Hz) of Free $P(OPh)_3$ (3) and of the Adduct Rh*←3 (1:1 molar ratio of the components), and Adduct Formation Shifts ($\Delta\delta$, in ppm), in $CDCl_3$

		free ligand		ligand in the adduct		
X		δ	$^nJ(^{31}P,X)$	δ	$^nJ(^{31}P,X)$	$\Delta\delta$
^{1}H	2/6	7.14	$^4J < 1.0$	7.00	n.d.[a]	n.d.
	3/5	7.31	$^4J < 1.0$	to	n.d.	n.d.
	4	7.12	$^4J < 1.0$	7.25	n.d.	n.d.
^{13}C	1	151.6	$^2J = 3.5$	151.1	$^2J \approx 0$	−0.5
	2/6	120.7	$^3J = 6.9$	120.5	$^3J \approx 0$	−0.2
	3/5	129.7	$^4J < 1.0$	129.1	$^4J \approx 0$	−0.6
	4	124.2	$^5J = 1.3$	124.7	$^5J \approx 0$	+0.5
^{31}P		129.2		8.0	$^1J_{RhP} = 143.1$ $^2J_{RhP} = 25.3$	−121.2

[a] n.d.: not determined due to signal overlap or signal complexity.

(11) Pretsch, E.; Bühlmann, P.; Affolter, C. *Structure Determination of Organic Compounds, Tables of Spectra Data*, 3rd ed.; Springer-Verlag: Berlin, Heidelberg, 2000.

Table 4. ^{1}H, ^{13}C, and ^{31}P Chemical Shifts (δ), Coupling Constants $^nJ(^{31}P,X)$ (in Hz) of Free Nonracemic 4 (S:R = 2.45:1) and of the Adduct Rh*←4 (1:1 molar ratio of the components),[a] Adduct Formation Shifts ($\Delta\delta$, in ppm), and Dispersion Effects [$\Delta\nu = \nu(R) - \nu(S)$, in Hz], in $CDCl_3$

		free ligand		ligand in the adduct			
X		δ	$^nJ(^{31}P,X)$	δ^b	$^nJ(^{31}P,X)$	$\Delta\delta$	$\Delta\nu$
^{1}H	1′	1.59	$^2J = 4.1$	2.13	$^2J = 9.9$	+0.54	+10.3
				2.11	$^2J = 10.7$	+0.52	
	2/6	7.45	$^3J = 7.6$	7.78	$^3J = 11.4$	+0.33	+16.3
				7.75	$^3J = 11.4$	+0.30	
	3/5	7.33	n.d.[c]	~7.26	n.d.	−0.07	~+33.0
				~7.19	n.d.	−0.14	
	4	7.35	$^5J \approx 1.5$	7.38	$^5J = 1.8$	+0.03	+20.8
				7.34	$^5J = 1.9$	−0.01	
	3″	6.85	$^4J = 4.1$	6.87	$^4J = 3.6$	+0.02	+29.6
				6.81	$^4J = 3.9$	−0.04	
	4″	7.30	$^5J \approx 1.5$	7.50	$^5J = 1-2$	+0.20	~0
				7.50	$^5J = 1-2$	+0.20	
	5″	6.91	$^4J < 1$	6.98	$^4J \approx 1.1$	+0.07	−18.5
				7.01	$^4J \approx 1.1$	+0.10	
	6″	7.03	$^3J \approx 7.6$	7.90	$^3J = 12.3$	+0.87	+31.4
				7.84	$^3J = 12.5$	+0.81	
	1‴	3.78	$^5J < 1$	3.46	$^5J \approx 0$	−0.32	+78.8
				3.30	$^5J \approx 0$	−0.48	
^{13}C	1′	11.1	$^1J = 13.2$	9.9	$^1J = 22.1$	−1.2	−30.1
				10.1	$^1J = 22.3$	−1.0	
	1	139.2	$^1J \approx 11.2$	n.d.			
	2/6	132.5	$^2J = 19.7$	131.5	$^2J = 10.6$	−1.0	−4.7
				131.5	$^2J = 10.3$	−1.0	
	3/5	128.3	$^3J = 7.0$	128.1	$^3J = 7.4$	−0.2	+9.5
				128.0	$^3J = 7.9$	−0.3	
	4	128.4	$^5J < 1$	129.5	$^4J = 2.4$	+0.8	−1.3
				129.6	$^4J = 2.6$	+0.9	
	1″	128.3	n.d.	118.8	$^1J = 33.1$	−9.5	+27.8
				118.5	$^1J = 34.5$	−9.8	
	2″	161.9	$^2J = 13.4$	161.5	$^2J = 0.5$	+0.6	−10.6
				161.6	$^2J = 1.9$	+0.7	
	3″	110.2	$^3J = 1.4$	111.5	$^3J = 3.8$	+1.3	+10.7
				111.4	$^3J = 4.1$	+1.2	
	4″	129.8	$^5J < 2$	132.6	$^4J = 2.2$	+2.8	+5.3
				132.6	$^4J = 2.4$	+2.8	
	5″	120.9	$^3J = 1.7$	120.8	$^3J = 9.8$	−0.1	+1.5
				120.8	$^3J = 9.4$	−0.1	
	6″	131.5	$^2J = 3.4$	n.d.			
	1‴	55.5	$^4J \approx 0$	55.1	$^4J \approx 0$	−0.5	+25.9
				54.9	$^4J \approx 0$	−0.7	
^{31}P		−34.3		−46.7	$^1J_{RhP} = 105.7$	−12.4	104.1
					$^2J_{RhP} = 22.2$		
				−47.2	$^1J_{RhP} = 102.2$	−12.9	
					$^2J_{RhP} = 20.7$		

[a] Dispersions at MTPA-OCH_3: ^{1}H, $\delta = 2.95$ (R) and 2.93 (S), $\Delta\nu = 9.9$ Hz; ^{13}C, $\delta = 54.6_1$ (R) and 54.5_8 (S), $\Delta\nu = 3.1$ Hz. [b] For each entry, the upper value corresponds to the (R)- and the lower to the (S)-enantiomer. [c] n.d.: not determined due to signal overlap or signal complexity.

of an AA′XX′ spin system. The third molar equivalent of **1** finds no further rhodium sites, so that the ^{31}P signal of the free PPh_3 ($\delta = -4.2$) appears as an additional singlet (Figure 1, bottom). This result is remarkable in that a strong selectivity in forming the adducts exists depending on the availability of PPh_3 (**1**).[12] Moreover, it corresponds with previous reports for other dirhodium complexes with alkylated carboxylates[10] in the fact that no internal rearrangement (axial vs equatorial ligands; see below) takes place in **Rh*** adducts.

(12) This is in sharp contrast to the behavior of selenium ligands where the free **Rh*** complex ("0:1 adduct") and the 1:1- and the 2:1 adducts form fast dynamic equilibria: Rozwadowski, Z.; Malik, S.; Tóth, G.; Gáti, T.; Duddeck, H. *J. Chem. Soc., Dalton Trans.* **2003**, 375−379.

Table 5. ^{1}H, ^{13}C, and ^{31}P Chemical Shifts (δ), Coupling Constants $^nJ(^{31}P,X)$ (in Hz) of Free *rac*-5 and of the Adduct Rh*←5 (1:1 molar ratio of the components),[a] Adduct Formation Shifts ($\Delta\delta$, in ppm), and Dispersion Effects ($\Delta\nu$, in Hz, at 11.74 T), in $CDCl_3$

		free ligand		ligand in the adduct			
X		δ	$^nJ(^{31}P,X)$	δ	$^nJ(^{31}P,X)$	$\Delta\delta$	$\Delta\nu^b$
^{1}H	1′	1.49	$^2J = 5.6$	1.99	$^2J = 9.7$	+0.50	1.7
	1″	3.02	$^3J = 9.7$	3.30	$^3J = 9.2$	+0.28	<1
		3.00	$^3J = 9.7$	3.28	$^3J = 9.2$	+0.28	
	2″	1.08	$^4J \le 0.5$	1.08	$^4J \le 0.5$	+0.00	<1
	2/6	7.37	$^3J \approx 10$	7.79	$^3J \approx 9$	+0.42	~9
				7.77	$^3J \approx 9$	+0.40	
	3/5	7.32	$^4J \approx 2$	≈ 7.23	n.d.[c]	~−0.09	n.d.
	4	7.23	$^5J < 1$	7.35	$^5J \approx 1$	+0.13	~1
^{13}C	1′	14.1	$^1J = 18.2$	11.6	$^1J = 17.8$	−2.5	72.6
				11.1	$^1J = 15.6$	−3.0	
	1″	43.7	$^2J = 14.6$	41.8	$^2J = 2.9$	−1.9	28.4
				41.6	$^2J = 1.9$	−2.1	
	2″	15.2	$^3J = 3.1$	14.5	$^3J = 3.1$	−0.7	18.2
				14.4	$^3J = 3.1$	−0.8	
	1	144.5	$^1J = 14.6$	134.6	$^1J = 34.8$	−9.9	25.9
				134.4	$^1J = 36.7$	−10.1	
	2/6	129.5	$^2J = 16.1$	131.3	$^2J = 10.3$	+1.8	0.9
				131.2	$^2J = 10.3$	+1.7	
	3/5	128.0	$^3J = 4.1$	128.3	$^3J = 9.6$	+0.3	5.2
				128.3	$^3J = 9.4$	+0.3	
	4	127.2	$^4J = 1.0$	130.0	$^4J = 2.4$	+2.8	2.5
				130.0	$^4J = 2.6$	+2.8	
^{31}P		49.9		11.5	$^1J_{RhP} = 106.2$	−38.4	106.5
					$^2J_{RhP} = 21.5$		
				11.0	$^1J_{RhP} = 106.2$	−38.9	
					$^2J_{RhP} = 23.0$		

[a] Dispersions at MTPA-OCH_3: ^{1}H, $\delta = 2.99$ and 2.97, $\Delta\nu = 12.1$ Hz; ^{13}C, $\delta = 54.6_0$ and 54.5_6, $\Delta\nu = 4.0$ Hz. [b] n.d.: not determined due to signal overlap or signal complexity.

Table 6. ^{1}H, ^{13}C, and ^{31}P Chemical Shifts (δ), Coupling Constants $^nJ(^{31}P,X)$ (in Hz) of Free *rac*-6 and of the Adduct Rh*←6 (1:1 molar ratio of the components),[a] Adduct Formation Shifts ($\Delta\delta$, in ppm), and Dispersion Effects ($\Delta\nu$, in Hz, at 11.74 T), in $CDCl_3$

		free ligand		ligand in the adduct			
X		δ	$^nJ(^{31}P,X)$	δ	$^nJ(^{31}P,X)$	$\Delta\delta$	$\Delta\nu$
^{1}H	1′	1.78	$^2J = 8.4$	2.36	$^2J = 8.5$	+0.58	~0
			$^5J_{FH} = 1.0$		$^5J_{FH} = 2.5$		
	1″	3.57	$^3J = 14.5$	4.00	$^3J = 13.5$	+0.43	8.1
				3.99		+0.42	
^{13}C	1′	17.4	$^1J = 16.7$	14.5	$^1J = 16.0$	−2.9	5.8
			$^4J_{FC} = 4.3$	14.5	$^1J = 15.1$	−2.9	
	1	115.3	$^1J = 59.7$	107.2	n.d.[b]	−8.1	n.d.
			$^2J_{FC} = 22.3$				
	2/6	137.4	n.d.	137.7	n.d.	+0.3	n.d.
			$^1J_{FC} = 253.4$		$^1J_{FC} \approx 247.6$		
	3/5	147.0	$^3J = 10.6$	146.5	n.d.	−0.5	n.d.
			$^1J_{FC} = 246.7$		$^1J_{FC} \approx 251.5$		
	4	142.2	$^4J \approx 0$	142.8	n.d.	+0.6	n.d.
			$^1J_{FC} = 255.8$		$^1J_{FC} \approx 264.1$		
			$^2J_{FC} = 13.4$				
			$^3J_{FC} = 5.5$				
	1″	57.2	$^2J = 17.8$	56.5	$^2J = 11.0$	−0.7	<2.0
			$^5J_{FC} = 0.7$				
^{31}P		119.1	$^3J_{PF} = 32.5$	58.0	$^1J_{RhP} = 114.2$	−61.1	34.5
			$^4J_{PF} = 2.6$		$^2J_{RhP} = 33.2$		
				57.4	$^1J_{RhP} = 114.7$	−61.7	
					$^2J_{RhP} = 33.6$		

[a] Dispersions at MTPA-OCH_3: ^{1}H, $\delta = 3.07$ and 3.05, $\Delta\nu = 6.3$ Hz; ^{13}C, $\delta = 54.6_2$ and 54.6_0, $\Delta\nu = 1.7$ Hz. [b] n.d.: not determined due to signal overlap or signal complexity.

It should be noted that in the respective titration experiments the adducts can be monitored by the

Table 7. ^{1}H, ^{13}C, and ^{31}P Chemical Shifts (δ), Coupling Constants $^{n}J(^{31}P,X)$ (in Hz) of the Free *rac*-7 and of the Adduct Rh*←7 (1:1 molar ratio of the components),[a] Adduct Formation Shifts ($\Delta\delta$, in ppm), and Dispersion Effects ($\Delta\nu$, in Hz, at 11.74 T), in $CDCl_3$

		free ligand		ligand in the adduct			
X		δ	$^{n}J(^{31}P,X)$	δ	$^{n}J(^{31}P,X)$	$\Delta\delta$	$\Delta\nu$
^{1}H	1′	1.73	$^{2}J = 8.6$	2.37	$^{2}J = 8.9$	+0.64	11.8
			$^{5}J_{FH} = 0.7$	2.35	$^{5}J_{FH} = 2.5$	+0.62	
	1″	4.04	$^{3}J = 9.6$	5.01	$^{3}J = 10.3$	+0.97	23.9
			$^{6}J_{FH} = 0.5$		$^{3}J_{HH} = 6.0$		
			$^{3}J_{HH} = 6.2$	4.96	$^{3}J = 10.3$	+0.92	
					$^{3}J_{HH} = 6.0$		
	2a″	1.27-a	$^{3}J_{HH} = 6.2$	1.33	$^{3}J_{HH} = 6.2$	0.06	24.7
			$^{4}J \approx 0$		$^{4}J \approx 0$		
				1.28	$^{3}J_{HH} = 6.2$	+0.01	
					$^{4}J \approx 0$		
	2b″	1.16-b	$^{3}J_{HH} = 6.2$	1.27	$^{3}J_{HH} = 6.2$	+0.11	11.5
			$^{4}J \approx 0$		$^{4}J \approx 0$		
				1.25	$^{3}J_{HH} = 6.2$	+0.09	
					$^{4}J \approx 0$		
^{13}C	1′	18.3	$^{1}J = 18.3$	16.1	$^{1}J \approx 11.0$	−2.2	<7.0
			$^{4}J_{FC} = 4.0$	16.0		−2.3	
	1	116.7	$^{1}J = 57.6$	107.9	n.d.[b]	−8.8	n.d.
			$^{2}J_{FC} = 18.2$		n.d.		
	2/6	137.3	n.d.	137.6	n.d.	+0.3	n.d.
			$^{1}J_{FC} = 253.4$		$^{1}J_{FC} \approx 253.6$		
	3/5	147.0	$^{3}J = 10.6$	146.6	n.d.	−0.4	n.d.
			$^{1}J_{FC} = 246.8$		$^{1}J_{FC} \approx 251.8$		
	4	142.1	$^{4}J \approx 0$	142.8	n.d.	+0.7	n.d.
			$^{1}J_{FC} = 255.5$		$^{1}J_{FC} \approx 253.0$		
			$^{2}J_{FC} = 13.4$		n.d.		
			$^{3}J_{FC} = 5.5$		n.d.		
	1″	74.3	$^{2}J = 20.9$	75.3	$^{2}J < 2.0$	+1.0	<2.0
	2a″	24.0-a	$^{3}J = 6.7$	24.6	$^{3}J = 1.4$	+0.6	∼0
	2b″	23.8-b	$^{3}J = 5.5$	24.1	$^{3}J = 6.5$	+0.3	∼0
				24.1	$^{3}J = 6.7$	+0.3	∼0
^{31}P		106.3	$^{3}J_{PF} = 36.4$	50.9	$^{1}J_{RhP} = 114.1$	−55.4	124.5
			$^{4}J_{PF} = 2.2$		$^{2}J_{RhP} = 29.3$		
				50.3	$^{1}J_{RhP} = 114.2$	−56.0	
					$^{2}J_{RhP} = 30.1$		

[a] Dispersions at MTPA-OCH_3: ^{1}H, $\delta = 3.06$ and 3.05, $\Delta\nu = 3.4$ Hz; ^{13}C, $\delta = 54.5_6$ and 54.5_5, $\Delta\nu = 0.7$ Hz. [b] n.d.: not determined due to signal overlap or signal complexity.

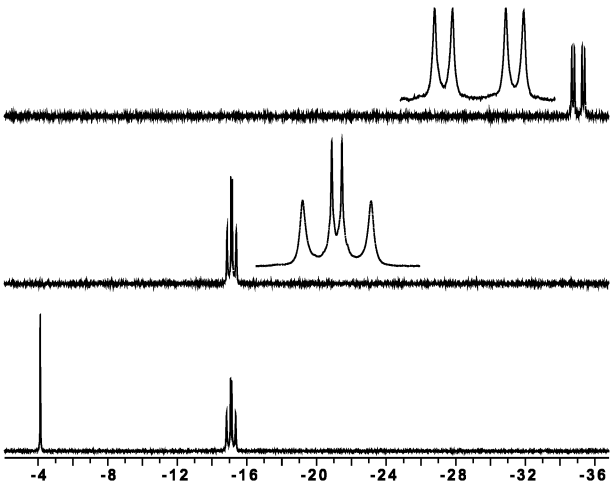

Figure 1. ^{31}P signals of PPh_3 (**1**) in the presence of **Rh***. Molar ratio **1**:**Rh*** is 1:1 (top), 2:1 (center), and 3:1 (bottom). Insets are signal expansions.

observation not only of the ^{31}P signals (Figure 1) but also the methoxy ^{1}H signals of **Rh*** (Figure 2): free **Rh*** ("0:1 adduct"), $\delta = 3.19$; 1:1 adduct, $\delta = 2.82$; 2:1 adduct, $\delta = 2.55$.

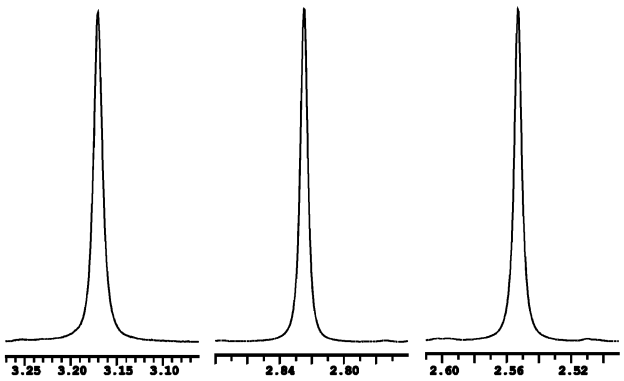

Figure 2. ^{1}H signals of methoxy groups in **Rh***. Molar ratios **1**:**Rh*** are 0:1 (left), 1:1 (center), and 2:1 (right).

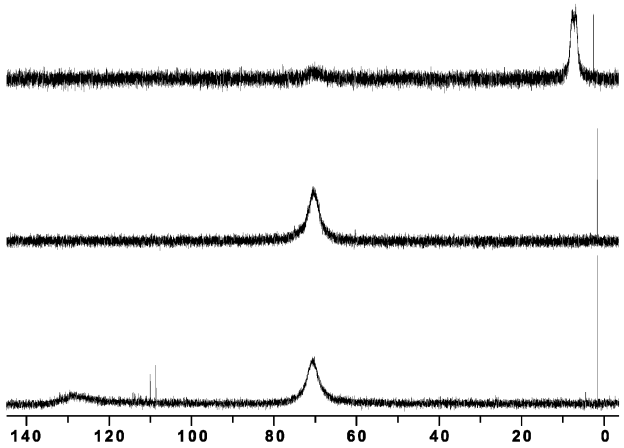

Figure 3. ^{31}P signals of $P(OPh)_3$ (**3**) in the presence of **Rh***. Molar ratio **1**:**Rh*** is 1:1 (top), 2:1 (center), and 3:1 (bottom).

The situation is analogous for triphenyl phosphite (**3**) except the following (Figure 3): (a) the NMR parameters of **3** are, of course, different from those of **1** (Table 3); (b) significant signal broadening due to coalescence is observed; the exchange rate is much higher than for **1**; (c) the selectivity between the different types of adducts is much less pronounced than for **1**; the corresponding $\Delta\Delta G°$ value is −3 to −3.5 kJ mol^{-1}, as estimated from the signal intensities in Figure 3 (top, rhodium site excess). Thus, the use of **Rh*** for chiral recognition of phosphines will not be handicapped by the appearance of various isomeric adducts showing an unpredictable variety of NMR peaks.

Telser and Drago[10] performed analogous experiments with the dirhodium complex $Rh_2(O_2CCF_3)_4$ (**Rh-TFA**). So, we repeated them in a similar although not identical way. Drago et al. prepared their samples by adding phosphine solutions dropwise to a **Rh-TFA** solution (both in toluene), until a 2:1 molar ration was achieved, and subsequently they removed the solvent and recrystallized the adducts before low-temperature NMR measurement (223 K).[10] In our procedure, however, portions of 1 molar equiv of the pure phosphine were added three times to the **Rh-TFA** solution in $CDCl_3$ consecutively, each time followed immediately by a room-temperature NMR measurement. The results of our experiments deviate significantly from those with **Rh***:

In the first step of adding PPh_3 (**1**) to **Rh-TFA** (1:1 molar ratio; Figure 4, top) the 1:1 adduct ($\delta = -35.6$) was formed selectively. This is in analogy with the

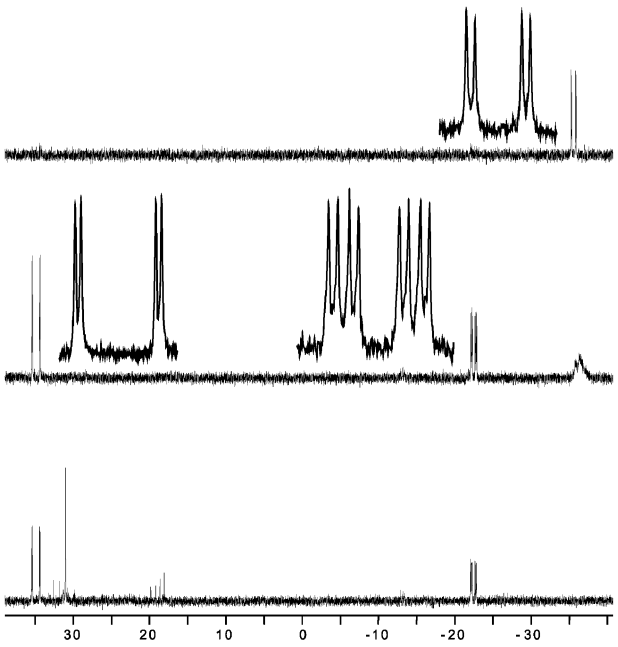

Figure 4. ^{31}P signals of PPh_3 (**1**) in the presence of **Rh-TFA**. Molar ratio **1**:**Rh-TFA** is 1:1 (top), 2:1 (center), and 3:1 (bottom). Insets are signal expansions.

experiment using **Rh***. However, the addition of the second molar equivalent of PPh_3 had a different effect (Figure 4, center): whereas some 1:1 adduct still remains, two new signals appear at $\delta(^{31}P) = -22.5$ with $^1J(^{103}Rh,^{31}P) = 93.1$, $^2J(^{103}Rh,^{31}P) = 27.5$ Hz, and $J(^{31}P,^{31}P) = 12.1$ Hz and at $\delta(^{31}P) = +34.9$ with $^1J(^{103}Rh,^{31}P) = 165.2$, $^2J(^{103}Rh,^{31}P) \approx 0$, and $J(^{31}P,^{31}P) = 11.9$ Hz. This corresponds well with Drago's results (ABXY)[10b] and further supports his interpretation proposing the existence of a class II adduct[10,13] with one axial and one equatorial phosphine ligand. Drago's third peak at $\delta(^{31}P) = -15.1$, however, which was ascribed to the "regular" 2:1 adduct with two axial phosphines (class I), is missing in our experiment; possibly, it may correspond to a very minute signal at $\delta(^{31}P) \approx -13$ in our spectrum. Finally, when the third molar equivalent of **1** is added (Figure 4, bottom), the signal of the 1:1 adduct disappears, and the third mole of **1** is completely consumed for new class II adduct formation.

A further signal appears at $\delta = +31.0$ as a singlet, the chemical shift of which was practically identical with that of separately added triphenylphosphine oxide ($Ph_3P{=}O$). Thus, this oxide is formed by air oxidation of **1** during the NMR experiment. It has been noted before that phosphines are easily oxidized when complexed to rhodium atoms.[10]

Again, a fast dynamic behavior can be seen for $P(OPh)_3$ (**3**) in the presence of **Rh-TFA** (Figure 5), where the ^{31}P signals of the "regular" 1:1 and the 2:1 adducts (class I) are very broad and do not show any splitting (Figure 5, center); this is due to intermolecular ligand exchange. Addition of the second molar equivalent of **3** (Figure 5, center), however, produces a new signal at $\delta(^{31}P) = +109.3$ with $^1J(^{103}Rh,^{31}P) = 215.0$ Hz as a sharp doublet. Apparently, there is no exchange like that observed for the other signals; the existence of only one

(13)) Girolami, G. S.; Mainz, V. V.; Andersen, R. A. *Inorg. Chem.* **1980**, *19*, 805−810.

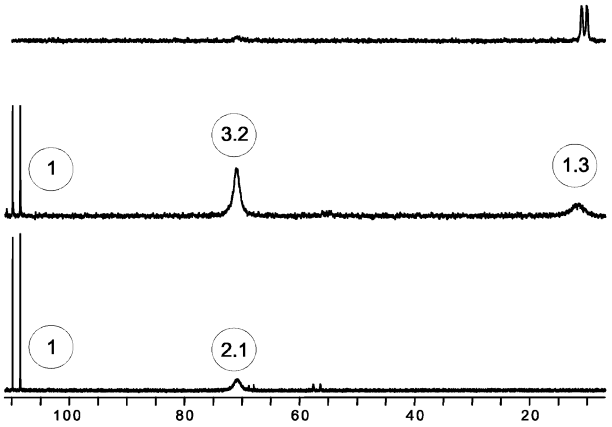

Figure 5. ^{31}P signals of $P(OPh)_3$ (**3**) in the presence of **Rh-TFA**. Molar ratio **1**:**Rh-TFA** is 1:1 (top), 2:1 (center), and 3:1 (bottom). The encircled values are relative signal intensities.

Scheme 2. Structures of the Chiral Phosphines 4−7

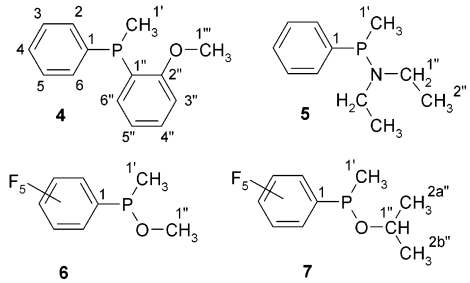

large $^{103}Rh-^{31}P$ coupling suggests a breaking of the Rh−Rh bond and formation of a monorhodium complex (compare also ref 10b). After the third molar equivalent (Figure 5, bottom) no 1:1 adduct is left, but, as expected, the relative amount of the "monorhodium complex" is enhanced, as can be seen from the relative signal intensities (encircled numbers).

(II) NMR Parameters of the Chiral Phosphines: Discrimination of Enantiomers. For this investigation we chose different types of chiral phosphines (Scheme 2; all racemates except **4**; see Experimental Part).

Adduct Formation Shifts and Coupling Constants. The chiral phosphine **4** shows a behavior similar to that of PPh_3 (**1**) in an NMR titration experiment (Figure 6). However, it seems that pure 2:1 adducts are formed only if the molar ratio **4**:**Rh*** clearly exceeds 2:1. Adding the second molar equivalent of **4** (Figure 6, center) leads to the production of a small amount of a decomposition product ($\delta = +36.5$, doublet), probably analogous in structure to the monorhodium complex (Figure 5), and still leaves a small proportion of the 1:1 adduct behind. Addition of the third molar equivalent of **4** finally ends in the exclusive 2:1 adduct accompanied by minor amounts of the above-mentioned decomposition product plus another similar one accompanied by the *P*-oxide of **4** ($\delta = +29.8$, singlet; slowly produced by air oxidation; see above).

The NMR data in Table 4 correspond to the 1:1 adduct of **4**; the diastereomeric adducts could be differentiated because **4** is nonracemic; note the intensity difference in the ^{31}P signals of the 1:1 adducts (two partially

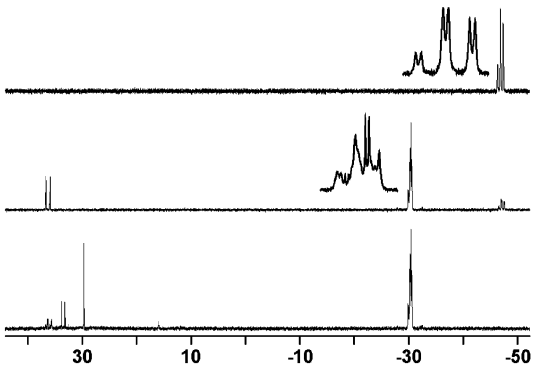

Figure 6. ^{31}P signals of nonracemic **4** in the presence of **Rh***. Molar ratio **4**:**Rh*** is 1:1 (top), 2:1 (center), and 3:1 (bottom). Insets are signal expansions.

overlapping doubled doublets in Figure 6, upper right). Analogously, 1:1 adducts of the racemic phosphines **5**−**7** were prepared and studied; their data are compiled in Tables 5−7.

As expected, ^{1}H and ^{13}C chemical shifts are moderately or hardly affected by adduct formation; most $\Delta\delta$ values (chemical shift differences in 1:1 adducts relative to the respective free phosphine ligands) are below 1 ppm except a few carbon atoms: the *ipso*-carbons attached to P (C-1) experience shieldings of 7−10 ppm, and the methyl carbons of **5** to **7** (C-1′) as well as a few further aliphatic and aromatic carbons show shieldings in the range of 2−3 ppm (see Tables 4−7). Phosphorus atoms are significantly shielded, and the nature of the substituents plays an important role; the following $\Delta\delta$(^{31}P) values are observed: **1**/**2**, −31.1; **3**, −121.2; **4**, −12.3 (*R*)/−12.9 (*S*); **5**, −38.4/−38.9; **6**, −61.1/−61.7; **7**, −55.4/−56.0. A dependence on the number and the nature of electronegative substituents at P is apparent, but the trend is not straightforward. The shielding of ^{31}P can be explained by electronic interaction between phosphorus and the electropositive Rh(II) atoms. We found analogous trends for ^{77}Se chemical shifts in selenoethers[14] and phosphine selenide ligands.[5f]

Significant changes of coupling constants involving ^{31}P and ^{1}H or ^{13}C, respectively, are scarce. Only one-bond ^{31}P,^{13}C couplings for *ipso*-carbons (C-1) are sometimes enhanced up to their 2- or even 3-fold magnitude by adduct formation. In this context it should be noted that ^{4}J(^{31}P,^{19}F) coupling constants in the free ligands **6** and **7** (2.6 and 2.2 Hz, respectively) give rise to a triplet splitting of the ^{31}P signal. In the adduct, however, this coupling seems not to exist (<0.5 Hz). Both evidences, enormous changes in ^{1}J(^{31}P,^{13}C) and vanishing of ^{4}J(^{31}P,^{19}F), may point to a common source: AM1 calculations of the free ligands **6** and **7** predict relaxed conformations in which the phenyl and pentafluorophenyl groups are coplanar with respect to the free electron pair at P, the HOMO of these phosphines (Scheme 3, top). In the adduct, however, one of the *ortho*-H or -F, respectively, would be in steric conflict with the nearby Mosher acid residues in **Rh*** (adduct formation via the n_P orbital). Therefore, the phenyl/pentafluorophenyl group is expected to rotate around the P−C bond (Scheme 3, bottom), thereby avoiding spatial interference and influencing the mechanisms in the mentioned

(14) Malik, S.; Moeller, S.; Tóth, G.; Gáti, T.; Choudhary, M. I.; Duddeck, H. *Magn. Reson. Chem.* **2003**, *41*, 455−465.

Scheme 3. Preferred Conformation of Free 6 as Calculated by AM1 (top) and Expected Conformational Change in the Adduct (bottom)

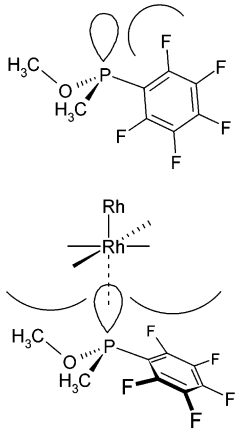

coupling pathways by changing the relative spatial orientation of the n_P orbital and π-system.

One-bond ^{103}Rh,^{31}P coupling constants depend on the number of heteroatoms directly attached to P and their electronegativity. Whereas phosphines with three attached carbon atoms (**1**, **2**, and **4**) show values of ca. 100 Hz or slightly lower, one nitrogen (**5**) increases the *J* values to 106 Hz and one oxygen (**6** and **7**) to 114−115 Hz. In the phosphite **3** with its three oxygen atoms the coupling constant is as high as 143 Hz. In contrast, two-bond ^{103}Rh,^{31}P coupling constants span a smaller range (20.8−33.6 Hz), but no obvious dependence on the substituents' nature can be derived here.

Diastereomeric Dispersions. Dispersion values $\Delta\nu$ are chemical shift differences (in Hz) of respective atoms in diastereomeric 1:1 adducts. They are often significant here; especially for the ^{31}P nuclei large signal splittings up to ca. 120 Hz exist (see Tables 4−7). Thus, the determination of enantiomeric ratios of the phosphine ligands is very easy by recording ^{31}P NMR spectra, although it should be recognized that each signal is a double doublet due to the ^{103}Rh,^{31}P couplings. A more detailed discussion on $\Delta\nu$ values of the 1:1 adduct **5**→**Rh*** has been reported by us before.[9]

The ^{1}H NMR spectra of nonracemic **4** (*S*:*R* = 2.45:1) in the presence of various molar ratios of **Rh*** deserve special attention because they allow a deep insight into the stereochemistry of the adducts. As shown before (Figure 6), only 1:1 adduct molecules exist in an equimolar ratio, similar to what was observed for triphenylphosphine (**1**). Figure 7, top, shows a section of the respective ^{1}H NMR spectrum.

The methoxy signals of **4** (in the anisyl residues, Figure 7, left) appear as two singlets at δ = 3.46 [(*R*)-**4**→[**Rh**-**Rh**]$^{(R)}$] and 3.30 [(*S*)-**4**→[**Rh**-**Rh**]$^{(R)}$]. The dispersion $\Delta\nu$ [=ν(*R*) − ν(*S*); at 11.74 T; 500.1 MHz] due to the existence of the two diastereomeric 1:1 adducts is +78.8 Hz, an exceedingly large value. This dispersion is due to the different interaction between **Rh*** (with Mosher acids being exclusively in *R*-configuration) and the *R*- or *S*-configured **4**, respectively. The methoxy signals of the Mosher acid residues reflect the existence of the two adducts as well, resonating at δ = 2.95 [(*R*)-**4**→[**Rh**-**Rh**]$^{(R)}$] and 2.93 [(*S*)-**4**→[**Rh**-**Rh**]$^{(R)}$] ($\Delta\nu$ = +9.9 Hz).

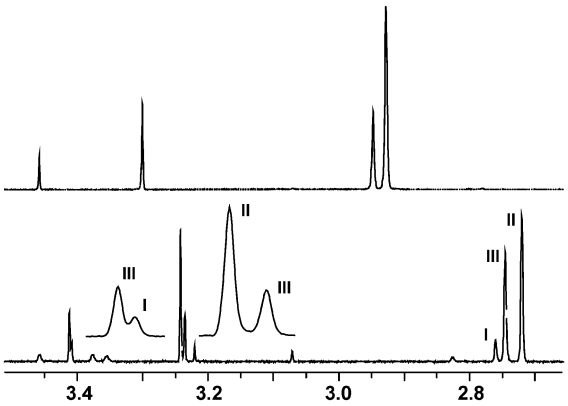

Figure 7. Methoxy ^{1}H signal region of nonracemic **4** in the presence of **Rh***. Molar ratio **4**:**Rh*** is 1:1 (top) and 3:1 (bottom). Insets are signal expansions.

Scheme 4. Configurations of the Three Diastereomeric 2:1 Adducts of Rh* and 4[a]

(*R*)-**4**→[**Rh-Rh**]$^{(R)}$←(*R*)-**4** (**I**)

(*S*)-**4**→[**Rh-Rh**]$^{(R)}$←(*S*)-**4** (**II**)

(*R*)-**4**→[**Rh-Rh**]$^{(R)}$←(*S*)-**4**
≡ (**III**)
(*S*)-**4**→[**Rh-Rh**]$^{(R)}$←(*R*)-**4**

[a] The chiral dirhodium complex **Rh*** is represented by "[**Rh-Rh**]".

Turning to a ratio of 3:1 (Figure 7, bottom), we find signals of the 2:1 adduct exclusively; signals of the extra free ligand molecules are outside the range depicted. The methoxy groups of **4** in the diastereomeric adducts give rise to two signals at $\delta \approx 3.41$ [(*R*)-**4**] and 3.24 [(*S*)-**4**]; the $\Delta\nu$ value is now even larger than in the 1:1 adduct: ca. 86 Hz; again a consequence of different interactions between **Rh*** and the *R*- or *S*-configured. A closer look, however, shows that each signal appears twice (see insets in Figure 7); the signal at $\delta \approx 3.41$ shows a dispersion of 1.4 Hz and that at $\delta \approx 3.24$ one of 3.1 Hz. The explanation for this phenomenon is the fact that the protons in each methoxy group are capable not only of differentiating between the diastereomeric interaction of one (*R*)-**4** and (*S*)-**4** ligand molecule, respectively, with **Rh*** but also of recognizing the *P*-chirality of the second phosphine ligand at the backside of the 2:1 adduct molecule. The unequivocal assignment of these signals, based on their intensity distribution, to the three conceivable diastereomers **I**−**III** (Scheme 4) is given in Figure 7. For the first time, we find here a second type of chiral recognition transferring chirality information from one ligand molecule to the other. We assume that the interaction occurs via a modification of the conformational equilibria of the Mosher acid residues in the diastereomeric adducts, although it cannot be excluded that the P*−Rh−Rh−P* pathway is helical by a chiral distortion of the dirhodium tetraacylate core.

The ^{1}H signals of the Mosher acid methoxy groups (Figure 7, right) are more complex in the 2:1 adduct than in the 1:1 adduct as well. These protons, belonging to methoxy groups flanked by two *P*-chiral ligand molecules **4**, can recognize their chirality on both sides simultaneously. Their signals appear at $\delta = 2.76$, 2.74, and 2.72; the assignment to the three different diastereomeric 2:1 adducts **I**−**III**—as evident from the signal intensities—is given in Figure 7.

It is conspicuous that nearly all $\Delta\nu$ values of the ^{1}H signals of **4** are positive (Table 4); the only exceptions are H-5″ (−18.5) and the neighboring H-4″ (∼0). This leads to the speculation that the sign of ^{1}H dispersion effects may be indicative of the absolute configuration of phosphines and an empirical rule may be established. We performed a similar study in the case of some phenylselenenylmenthane derivatives,[15] however, without success because the $\Delta\nu$ signs were scattered and no trend was apparent. On the other hand, in the case of the phosphines the lifetimes of the adducts are much longer so that a more intimate contact between the ligand molecules and **Rh*** might exist. Currently, we are following this question by investigating more phosphine derivatives in order to see whether the results of **4** are solitary and accidental.

Conclusion and Experimental Conditions for the "Dirhodium Method"

In contrast to other ligands[5,7,12] phosphines form adducts with **Rh*** that are kinetically stable on the NMR time-scale so that the various types of adducts can be observed separately at room temperature.

As a result of this investigation, we can state that the optimal experimental setup for chiral recognition of phosphines using the "dirhodium method" is mixing the phosphine with **Rh*** in equimolar amounts so that 1:1 adducts with two axial phosphine ligands are formed predominantly, in the case of triorganylphosphines even exclusively.

The 2:1 adducts can easily be produced by mixing **Rh*** with 2 molar equiv of the phosphine, although the risk of some decomposition cannot be excluded. Chiral recognition is again possible, but three diastereomers exist instead of the two observed for the 1:1 adducts. This may give rise to three signals for the methoxy-^{1}H in the Mosher acid residues and even four for ligand atoms. In this case it is important for a safe determination of enantiomeric purity to rely on unequivocal signal assignments.

Using **Rh-TFA** in analogous comparative experiments may, however, produce considerable amounts of class II adducts,[10,13] and even decomposition products may emerge as soon as 1 molar equiv of phosphine is exceeded.

The number of heteroatoms (N or O) attached to the phosphorus in the phosphine ligands has a significant influence on the thermodynamic parameters in the adduct formation equilibria. As long as all atoms at P are carbons, the energy difference between 1:1 and 2:1 adducts is large enough (in favor of the 1:1 adduct) to produce both adducts separately in an NMR titration experiment. If, however, three oxygen atoms are attached to P, the exchange rate may become so large and the barrier so low that the NMR signals show coalescence effects at room temperature; either a temperature increase or decrease may be necessary. Moreover, **Rh***,

(15) Malik, S.; Moeller, S.; Duddeck, H.; Choudhary, M. I. *Magn. Reson. Chem.* **2002**, *40*, 659−665.

1:1, and 2:1 adducts may exist simultaneously over a wide range of molar ratios of the components.

Experimental Part

Syntheses. The synthesis of **Rh*** has been described before.[5a] The phosphines **1** and **2** as well as triphenyl phosphite (**3**) are commercially available. The phosphines **4**−**7** were synthesized as described below.

(2-Methoxyphenyl)methylphenylphosphine (4). To the solution of (2-methoxyphenyl)phenylphosphine oxide[16] (0.1 mol) and triethylamine (0.3 mol) in dry benzene (50 mL) was added dropwise trichlorosilane (0.3 mol). The reaction mixture was heated under reflux 6 h, then was cooled, and a solution of NaOH in water (∼50 mL, 25% w/w) was added dropwise with vigorous stirring. The organic layer was separated and washed with water (3 × 25 mL), dried ($MgSO_4$), and concentrated under reduced pressure. The resulting brown oil was distilled in vacuo to give a colorless oil that solidified on cooling. Yield: 95%, mp 46−47 °C (45−46 °C),[16] bp 104−110 °C/0.2 Torr.

***(S)*-(−)-(4).** This compound was obtained in 96% yield from (*S*)-(2-methoxyphenyl)methylphenylphosphine oxide by the published procedure;[17] $[\alpha]_D$ −38.2° (*c* 1.15, methanol), ∼93% ee ($[\alpha]_D$ 41°).[17] The sample used for the chiral recognition experiments was prepared by mixing (*S*)-(−)-(**4**) and *rac*-(**4**) so that an enantiomeric excess (ee) of 42% (*S*:*R* = 2.45:1) was obtained. IR ($\tilde{\nu}$, neat): 3062 (w), 2964 (w), 1584 (m), 1464 (s), 1429 (s), 1288 (m), 1270 (m), 1237 (s), 1131 (m), 1071 (m), 874 (s), 792 (m), 748 cm^{-1} (s). EIMS (70 eV): *m*/*z* 231 (53%) [M^+ + 1], 230 (100%) [M^+], 229 (99,9%), 211 (19%), 199 (71%), 197 (79%), 183 (63%), 165 (12%), 151 (15%), 139 (22%), 137 (30%), 124 (24%), 121 (23%), 109 (14%), 107 (18%), 91 (49%), 77 (18%), 65 (6%). High-resolution ESMS (MeCN−H_2O): *m*/*z* 231.0850 [M^+ + H], calcd for $C_{14}H_{16}OP$ 231.0939.

Compound **5** was prepared from (*N*,*N*-diethylamino)phenylchlorophosphine with methyllithium in diethyl ether analogously to a Grignard reagent as described by Bestmann et al.[18] (*N*,*N*-Diethylamino)phenylchlorophosphine was synthesized by the procedure given by Maier[19] from phenyldichlorophosphine and bis(*N*,*N*-diethylamino)phenylphosphine.

***(N,N*-Diethylamino)methylphenylphosphine (5).** Methyllithium (49.4 mL in hexane, 1.6 mol/L) was added dropwise to $PhP(NEt_2)Cl$ (17.1 g, 0.079 mol) in diethyl ether (200 mL) at −20 °C under argon. Then, the reaction mixture was warmed to room temperature. After 2 h the mixture was filtered, the solvents were evaporated, and the residue was distilled in vacuo (bulb-to-bulb distillation, oven temperature 95−100 °C/0.1 Torr) to give **5** (11.5 g, 74.2% yield; bp 100 °C/0.2 Torr[18]). IR ($\tilde{\nu}$, neat): 3070 (w), 2963 (m), 1586 (w), 1479 (w), 1462 (w), 1451 (w), 1433 (w), 1373 (m), 1292 (w), 1182 (s), 1093 (w), 1022 (s), 923 (m), 858 (m), 788 (m), 740 cm^{-1} (s). EIMS (70 eV): *m*/*z* 196 (9%) [M^+ + 1], 195 (67%) [M^+], 180 (100%), 166 (9%), 152 (41%), 140 (54%), 125 (68%), 123 (72%), 121 (35%), 109 (80%), 107 (24%), 104 (21%), 91 (15%), 77 (30%), 72 (20%), 70 (17%), 65 (7%).

Compounds **6** and **7** were prepared by a known condensation reaction of methyl(pentafluorophenyl)chlorophosphine with methanol or 2-propanol in the presence of triethylamine.

***O*-Methyl Methyl(pentafluorophenyl)phosphinite (6).** MeOH (0.26 g, 8 mmol) was added to methyl(pentafluorophenyl)chlorophosphine (1.5 g, 6 mmol) in diethyl ether (15 mL) at 0 °C. Then, triethylamine (0.83 g, 7.2 mmol) was added dropwise under nitrogen. After 10 h triethylamine hydrochloride was filtered off, the solvent was evaporated, and the residue was distilled in vacuo (0.2 Torr, temperature of distillation was not controlled) to give **6** (0.9 g, 61%). IR ($\tilde{\nu}$, neat): 2938 (w), 1638 (m), 1514 (s), 1463 (s), 1421 (m), 1378 (m), 1285 (m), 1179 (w), 1082 (s), 1037 (s), 972 (s), 892 (m), 872 (m), 823 cm^{-1} (m). EIMS (70 eV): *m*/*z* 244 (100%) [M^+], 229 (92%), 211 (14%), 199 (74%), 181 (6%), 163 (15%), 148 (11%), 143 (11%), 117 (10%), 111 (19%), 110 (15%), 93 (15%), 81 (33%), 77 (10%), 69 (20%), 65 (8%). High-resolution ESMS (MeCN−H_2O): *m*/*z* 245.0166 [M^+ + H], calcd for $C_8H_7F_5OP$ 245.0155.

***O*-Isopropyl Methyl(pentafluorophenyl)phosphinite (7).** Starting from methyl(pentafluorophenyl)chlorophosphine (1.75 g, 7.1 mmol), 2-propanol (0.45 g, 7.5 mmol), and triethylamine (0.72 g, 7.1 mmol), **7** (1.33 g, 69%) was obtained in the same manner as described for **6**. IR ($\tilde{\nu}$, neat): 2976 (m), 1638 (m), 1513 (s), 1466 (s), 1422 (m), 1381 (m), 1285 (m), 1175 (w), 1111 (m), 1082 (s), 963 (s), 893 (m), 865 (s), 824 (m), 757 cm^{-1} (w). EIMS (70 eV): *m*/*z* 272 (4%) [M^+], 252 (5%), 231 (12%), 230 (99,7%), 215 (100%), 213 (16%), 211 (13%), 181 (3%), 163 (4%), 148 (5%), 143 (5%), 110 (4%), 81 (5%), 69 (7%), 67 (20%), 65 (4%).

Spectroscopy. Room-temperature ^1H (400.1 MHz), ^{13}C (100.6 MHz), and ^{31}P (161.9 MHz) NMR measurements of the free ligands **1** and **3**−**5** (Schemes 1 and 2) and all titration experiments were performed on a Bruker DPX-400 spectrometer equipped with a QNP probe head. Room-temperature ^1H (500.1 MHz), ^{13}C (125.7 MHz), and ^{31}P (202.4 MHz) NMR measurements of the free ligands **1**, **2**, and **5**−**7** (Schemes 1 and 2) were performed on a Bruker DRX-500 spectrometer equipped with a broad-band inverse probe head.

TMS was used as internal standard for ^1H and ^{13}C ($\delta = 0$), aqueous H_3PO_4 ($\delta = 0$) for ^{31}P. Signal assignments are based on ^1H, ^{13}C, ^{31}P {^1H}, ^1H {^{31}P}, gs-^1H,^1H-COSY, gs-HMQC, gs-HSQC-edit, and gs-HMBC experiments (standard Bruker software). In the 1D NMR spectra, digital resolutions were 0.14 Hz/point for ^1H, 0.24 Hz/point for ^{13}C, and 0.22 Hz/point in the ^{31}P NMR spectra on the DRX-500 spectrometer; on the DPX-400 spectrometer the digital resolutions were 0.13 Hz/point for ^1H, 0.19 Hz/point for ^{13}C, and 0.7 Hz/point in the ^{31}P NMR spectra.

All samples were prepared by mixing 48.6 mg of **Rh*** (0.04 mmol) and the appropriate molar equivalent of the respective phosphine in 0.75 mL of $CDCl_3$, and 7.5 μL (1 drop) of acetone-d_6 was added to increase the solubility of **Rh***.[5d] Identical conditions were used for recording the spectra of the free ligands (absence of **Rh***).

IR spectra were recorded on an FT-IR spectrometer Vector 22 as pure compounds (ATR). Electron-impact MS spectra were recorded on a Finnigan MAT 312 at 70 eV and electrospray MS spectra on a Micromass LCT.

Acknowledgment. Valuable discussions with Prof. M. Chmielewski, Warsaw, Poland, concerning the stereochemistry of the adducts is gratefully acknowledged by H.D.; J.O. thanks the Alexander von Humboldt Foundation for a grant at the Technical University Braunschweig. The authors thank Dr. A. Karacar (Technical University Braunschweig) for a sample of methylpentafluorophenylchlorophosphine. This work has been performed within the project "Biologically Active Natural Products: Synthetic Diversity" (Department of Chemistry, Hannover University). It was supported by the Deutsche Forschungsgemeinschaft and the Polish Academy of Sciences, Warsaw.

OM0209529

(16) Mann, F. G.; Tong, B. P.; Wystrach, V. P. *J. Chem. Soc.* **1963**, 1155−1166.
(17) Knowles, W. S.; Sabacky, M.; Vineyard, B. D. *Homogeneous Catalysis II*, Adv. Ser. Chem. 1974; No. 132, p 274. Monsanto, US 4005127; *Chem. Abstr.* **1977**, *86*, 190463.
(18) Bestmann, H. J.; Lienert, J.; Heid, E. *Chem. Ber.* **1982**, *115*, 3875−3879.
(19) Maier, L. *Helv. Chim. Acta* **1963**, *46*, 2667−2676.